Int J Adv Manuf Technol (2017) 88:1383–1392
DOI 10.1007/s00170-016-8748-4

ORIGINAL ARTICLE

Pattern recognition in audible sound energy emissions of AISI 52100 hardened steel turning: a MFCC-based approach

Edielson P. Frigieri[1] · Tarcisio G. Brito[1] · Carlos A. Ynoguti[2] · Anderson P. Paiva[1] · João R. Ferreira[1] · Pedro P. Balestrassi[1]

Received: 17 January 2016 / Accepted: 5 April 2016 / Published online: 13 May 2016

Abstract The main objective in machining processes is to produce a high-quality surface finish which, however, can be measured only at the end of the machining cycle. A more preferable method would be to monitor the quality during the cycle, what result a real-time, low-cost, and accurate monitoring method that can dynamically adjust the machining parameters and keep the target surface finish. Motivated by this premise, results of investigation on the relationship between emitted sound signal and surface finish during turning process are reported in this paper. Through experiments with AISI 52100 hardened steel, this work shows that such a correlation does exist presenting strong evidences that Mel-Frequency Cepstral Coefficients, extracted from sound energy, can detect different surface roughness levels, what makes it a promising feature for real-time process quality monitoring methods.

Keywords Sound · Machining · Monitoring · Mel-frequency cesptral coefficients

✉ Edielson P. Frigieri
edielsonpf@unifei.edu.br

Carlos A. Ynoguti
ynoguti@inatel.br

[1] Industrial Engineering Institute, Federal University of Itajuba, 1303 BPS Avenue, Itajuba MG 37500-903, Brazil

[2] Electrical Engineering Department, National Institute of Telecommunication, 510 João de Camargo Avenue, Santa Rita do Sapucai MG 37540-000, Brazil

1 Introduction

Customers who need parts machined place a premium on the quality of surface finish [1]. Thus, to identify changes, failures, or tears in the machining process, researchers have studied and developed monitoring methods for many years, as can be seen in the overview presented by Teti et al. [2]. Sick [3] showed that monitoring methods can be classified as either direct or indirect, where direct methods analyze measurements of tool wear or surface roughness but carrying out of such methods must either interrupt the machining process or wait until its completion. Indirect methods however make use of other sources of information, such as, cutting forces [4], vibration signals [5], electric current, image [6], and many other sources. The great advantage of indirect methods is that they can be carried out without stopping or interfering with the machining process, thereby increasing efficiency and allowing online adjustments [7].

One indirect method that has recently attracted researchers attention concerns is the sound generated during the machining process [8–10] because using the produced sound to gauge information about machining process has two major advantages: ease of installation [8] and implemented at a lower cost than other sensors [11].

Some examples of investigations into the use of acoustic emissions to determine the status of processes and structures include, but are not limited to, Boutros and Liang [12], where a method based on sound signals allied to discrete HMM was proposed to detect and diagnose mechanical faults in machining processes and rotating machinery. In the case of cutting tool, the proposed method detected correctly three different states (i.e., sharp, worn, or broken). For bearing tests, the model classified the severity of the faults

seeded in two different engine bearings with a success rate greater than 95 %.

In another work based on sound signals collected in the milling process, Ai et al. [10] showed a relationship between each order component of LPCC and the flank wear, mainly concentrated in the sixth-, seventh-, and eighth-order components of LPCC. Correlating sound patterns and tool wear was carried out in another study by Mannan et al. [9] where authors concluded that tool condition can be monitored by combining sensory data from a microphone and a central composite design (CCD) camera.

Airborne sound was found by Robben et al. [13] to be a valuable source of information in an ongoing machining process for the cut-off grinding of concrete. The authors highlighted that because of the very high sound emission of the machining process in a controlled environment, there was no total influence of environmental noise on the proposed monitoring method.

Salgado and Alonso [14] proposed a tool condition monitoring system based on feed motor current and sound signal where Singular Spectrum Analysis (SSA) was used to extract information correlated with tool wear from the sound signal. Experiments using AISI 1040 steel showed that the proposed technique is fast and reliable for tool condition monitoring.

Lu and Wang [15] analyzed the high-frequency sound signals (range between 20 and 80 kHz) generated in micro-milling process and proposed a wear monitoring method. Results indicated that the normalized sound signals can be potentially applied in monitoring methods with the proper selection of feature bandwidth and other parameters.

Downey et al. [16] examined the feasibility of audible sound emissions in the frequency range spectrum of human hearing (between 0 and 20 kHz). They observed that it was possible to correlate the sound energy with tool wear in machining operations. Furthermore, audible acoustic spectra highlighted the possibility of identifying discrete phases in the cutting interface performance.

Most of presented works have focus on monitoring tool wear, and analysis of data that is offered by the machining process from the sensor configurations. As the objective of a machining process is the final quality of the workpiece, actually many efforts are directed to find efficient ways to monitor the quality of the machining process. Surface roughness raised as an important parameter for quality monitoring [17], as presented by [18], which proposed a dynamic surface roughness monitoring system based on artificial neural networks (ANN) achieving a success rate of 99 %.

Following this idea, the fundamental aim of this work is to determine if, instead of detecting tool wear, it is possible to identify differences in audible acoustic emissions for different finishing surface roughness levels and also if those differences are correlated with the machining cutting parameters, enabling its utilization in quality monitoring of machining process. Also, Mel-Frequency Cepstral Coefficients (MFCC) extracted from sound energy are used as acoustic spectrum features and their correlation with surface roughness are analyzed. MFCC is commonly used in other research areas, such as speech recognition [19, 20], but has not been explored for monitoring machining process, so this is the major contribution of this work.

The rest of the paper is organized as follows. The process of extracting acoustic features is presented in Section 2. In Section 3, the experiment is outlined showing all the steps for database creation. In Section 4, the obtained results are shown and also detailed in Section 5. Finally, conclusions and future work are given in Section 6.

2 Signal processing and feature extraction

2.1 Short-time fast Fourier transform

The sound that comes from the machining process is a dynamic signal: it varies with time due to small differences in the machined material, vibration, fluctuations in rotating speed, etc. Therefore, it is reasonable to consider it as a non-stationary signal and the use of classic FFT for analysis can loose the dynamic behaviors of all frequency components along the time. Such type of signal requires analysis in both time and frequency domain which can be achieved by the use of short-time Fourier transform (STFT), or spectrogram (power of STFT) [21, 22]. The STFT is based on the assumption that, during short time intervals, the signal can be considered stationary [23]. Therefore, the entire signal is divided into small successive overlapped frames multiplied by a non-zero window function, on which the FFT is applied [24].

According to [23], the STFT for a signal $s(t)$ can be expressed as

$$STFT(t,\omega) = \frac{1}{\sqrt{2\pi}} \int_{-\infty}^{+\infty} s(\tau) h(\tau - t) \mathrm{e}^{-j\tau\omega} \, \mathrm{d}\tau \qquad (1)$$

where $h(t)$ denotes a window function at time t. Window functions are used to avoid signal distortion and ensure a smooth transition from frame to frame of the estimated parameters [25]. A Hamming window was selected to be used in this paper.

Thus, the energy density at instant t can be calculated as

$$SPE(t,\omega) = |STFT(t,\omega)|^2 \qquad (2)$$

where $STFT(t,\omega)$ is obtained from Eq. 1.

As recorded data is a discrete signal, time instants are updated on a frame by frame basis where a frame consists of N_S samples of signal representing a time frame T_F. This

is the length of time (in seconds) over which a set of parameters is valid. Then the analysis moves T_W samples forward for a new frame k, and a new frame energy is calculated. It is important to notice that there is a superposition between adjacent frames. The amount of overlap to some extent controls how quickly parameters can change from frame to frame, which normally corresponds to an overlap of 50 % [25]. Finally, the result for each frame $k = 1, 2, ...K$, is a spectral energy vector $\overrightarrow{S_k}$ containing $N/2 + 1$ values of energy, where N corresponds to the number of FFT points. The total number of frames K depends on the selected frame interval (T_F) and time shift (T_W) besides the total signal length.

2.2 Mel-frequency cepstral coefficients

Depending on the size of N, a correlation analysis of all $N/2 + 1$ energy values with each machining parameter and also finishing surface roughness may not be satisfactory since many energy components tend to be auto-correlated. Also, this representation should remove as much irrelevant information as possible, for instance intensity, background noise, and retain only the information relevant for the signal classification. Thus, the acoustic vectors should attend the following requirements:

1. be of low dimensionality to allow a reliable estimation of the free parameters of the recognition system,
2. be independent of the recording environment, and
3. be characteristic for each machine setup, to allow an optimal discrimination between the different acoustic models.

One such parameter that has achieved a great success in this task is the MFCC feature, first proposed for the speech recognition problems [26]. It consists on a filter bank-based approach, which can be regarded as a crude model of the initial stages of transduction in the human auditory system [25].

There are two main motivations for the filter bank representation: first, the position of maximum displacement along the basilar membrane for stimuli such as pure tones is proportional to the logarithm of the frequency of the tone; second, experiments in human perception have shown that frequencies of a complex sound within a certain bandwidth of some nominal frequency cannot be individually identified. When one of the components of this sound falls outside this bandwidth, it can be individually distinguished. We refer to this bandwidth as the critical bandwidth [25]. A critical bandwidth is nominally 10 to 20 % of the center frequency of the sound.

The *Mel* scale attempts to map the perceived frequency of a tone onto a linear scale. It is often approximated as a linear scale from 0 to 1 kHz, and then a logarithmic scale beyond 1 kHz, and it is possible to define a mapping from the actual frequency f to a perceptual frequency scale by

$$f_{mel} = 2595 \log_{10}\left(1 + \frac{f}{700}\right). \tag{3}$$

The process for extracting the MFCC using this idea is outlined as follow. The first step is to calculate the energy spectrum of each frame k [19, 27] that is given by Eq. 2. Next, each energy frame S_k is filtered using a triangular filter bank, with the center frequencies (see Table 1) of each filter calculated by Eq. 3, resulting $\widetilde{s_k}$. The filtering process can be represented by

$$\widetilde{s_k}(l) = \sum_{j=0}^{N/2} S_k(j) M_l(j), \forall l = 1, 2, ..., L \tag{4}$$

where N is the number of FFT points and L is the number of *Mel* filters [6, 27].

Table 1 Central frequencies for a filter bank in *Mel* scale

Filter index	Center Freq. (Hz)	Filter index	Center Freq. (Hz)	Filter index	Center Freq. (Hz)
1	100	13	1516	25	8000
2	200	14	1741	26	9190
3	300	15	2000	27	10,556
4	400	16	2297	28	12,126
5	500	17	2639	29	13,929
6	600	18	3031	30	16,000
7	700	19	3482	31	18,379
8	800	20	4000	32	21,112
9	900	21	4595	33	24,251
10	1000	22	5278	34	27,858
11	1149	23	6063	35	32,000
12	1320	24	6964	36	36,758

Finally, a discrete cosine transform (DCT) is applied to the natural logarithm of the *Mel* spectrum, resulting in the mel-frequency Cepstral coefficients, as follows

$$c(m) = \sum_{i=0}^{L-1} \ln(\widetilde{s_k}(i)) \cos\left(\frac{\pi m}{2L}(2i+1)\right) \quad (5)$$

where $m = 1, 2, ..., C$ and C is the number of desired coefficients [28, 29]. Since most of the signal information is represented by the first coefficients, normally C is chosen between 12 and 20.

3 Experimental outline

3.1 Experimental setup

The experimental setup is based on a CNC lathe with a maximum rotational speed of 4000 rpm and power of 5.5 kW and using Wiper mixed ceramic (Al2O3+TiC) inserts (ISO code CNGA 120408S01525WH) coated with a very thin layer of titanium nitride (TiN; Sandvik-Coromant GC 6050). The workpieces were made of AISI 52100 steel with dimensions of 49–50 mm and a hardness between 49 and 52 HRC, up to a depth of 3 mm below the surface. Figure 1 detail the actual experimental setup, the location of microphone in relation to cutting interface and the tool holding configuration.

Surface roughness was measured using a Mitutoyo portable roughness meter model Surftest SJ 201, fixed to a cut-off length of 0.25 mm. The sound emissions were recorded using an audio microphone connected to the soundcard of a Dell Vostro laptop, using the software Audacity [30], configured for a sample frequency of 44.1 kHz with a resolution of 16 bits.

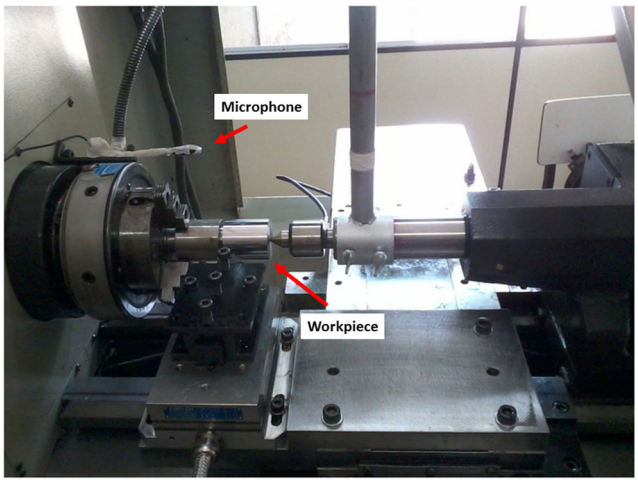

Fig. 1 Machining setup

3.2 Experimental methodology

CCD was used to determine the machining operational parameter values and to create a sequential set of experimental runs [31]. Due to the number of tools available for the experiment, 10 sets of machining parameters were selected based on D-optimality criteria [32]. Table 2 shows the resulted values for each experimental run considering cutting speed ($CS\ m/min$), feed rate ($F\ mm/rev$), depth of cut ($D\ mm$) and material removal rate (MRR).

During the experiment, it was guaranteed that there were no other machining operations taking place in the vicinity, which might have added interfering acoustic components and compromise the signals being detected. Each row of Table 2 was replicated 15 times to guarantee the statistical reliability of the experiment, resulting a total of 150 experimental runs. For each execution, sound signal was recorded and the following surface roughness parameters were measured: arithmetic average surface roughness (Ra), maximum surface roughness (Ry), root mean square roughness (Rq), 10-point height (Rz), and maximum peak to valley (Rt), measured three times at four positions in the work-piece middle, as proposed by [31]. From these results, the mean and variance were calculated for each surface roughness obtained. For each experimental cycle, the only change was the replacement of the cutting tool insert with an identical in order to guarantee the same wear condition.

4 Results

As outlined measurements of the surface finish of the workpiece were taken regularly during the experimental cycles to

Table 2 D-Optimal design for hard turning of AISI 52100 steel

Machining Setup	*CS*	*F*	*D*	*MRR*
Ms1	200.00	0.10	0.10	2.00
Ms2	240.00	0.10	0.10	2.40
Ms3	200.00	0.20	0.10	4.00
Ms4	200.00	0.10	0.20	4.00
Ms5	240.00	0.10	0.20	4.80
Ms6	240.00	0.20	0.20	9.60
Ms7	186.36	0.15	0.15	4.19
Ms8	220.00	0.23	0.15	7.72
Ms9	220.00	0.15	0.23	7.72
Ms10	220.00	0.15	0.15	4.95

Table 3 Surface roughness average for all machining setups

Machining setup	Surface roughness					
	Ra	*Ry*	*Rz*	*Rq*	*Rt*	*Rsm*
Ms1	0.15	1.05	0.75	0.18	1.44	85.60
Ms2	0.16	1.17	0.81	0.20	1.56	91.30
Ms3	0.44	2.39	1.76	0.53	3.09	169.72
Ms4	0.19	1.36	1.00	0.24	1.80	58.91
Ms5	0.18	1.32	0.89	0.23	1.89	100.67
Ms6	0.52	2.90	2.24	0.63	3.41	195.46
Ms7	0.26	1.87	1.25	0.33	2.71	104.31
Ms8	0.50	2.62	2.06	0.60	3.10	212.34
Ms9	0.26	1.90	1.29	0.33	2.70	73.04
Ms10	0.19	1.42	0.97	0.24	2.10	88.14

evaluate the performance of the cutting operation and also correlate with sound energy. Table 3 shows the average of 15 replicas for all surface roughness parameters resulted for each experimental run.

Samples in the range of 7 to 10 seconds duration were taken from the audio data for all experimental trials. The sample time range was chosen considering just the stable cutting period avoiding moments when cutting tool enters and exits of the work-piece [16], as illustrated by Fig. 2.

Energy frames was obtained from audio data using $N = 1024$ FFT points, a frame length of 20 ms and frame shift of 10 ms, that are common values used in speech analysis [27] and also have been applied in machining monitoring methods [10]. For each frame, $C = 12$ Mel-frequency Cepstral Coefficients were calculated using $L = 31$ filters which resulted a total of $K = 900$ energy vectors (on average).

Differently then expected, MFCC level distribution presented a stochastic behavior along time what reflected directly to the MFCC behavior. The same behavior was noted for all audio data, as can be seen in some examples on Fig. 3. Based on that, instead of using all $K = 900$ frames, it was calculated a mean and a standard deviation vector to represent each audio data. Therefore, the MFCC of each machining setup can be represented by $\overrightarrow{c_m} = (\overrightarrow{\mu_m}, \overrightarrow{\sigma_m})$, where $\overrightarrow{\mu_m}$ and $\overrightarrow{\sigma_m}$ are the mean and standard deviation of all K frames for each coefficient $m = 1, 2, ...C$, respectively, composed by $C = 12$ MFCC levels each.

5 Discussion of results

Correlation analysis was applied to identify which Mel-Frequency Cesptral Coefficient have strongly correlation

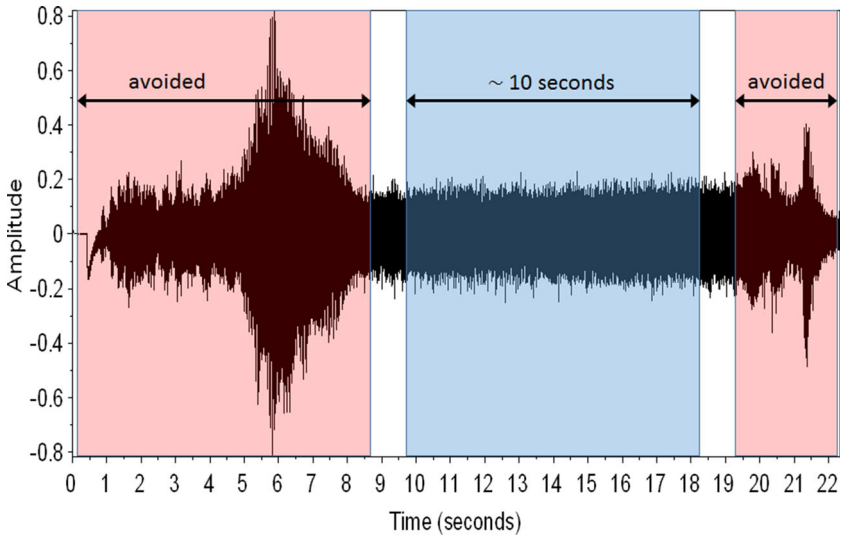

Fig. 2 Full audio recorded during machining ($CS = 200$, $F = 0.10$ and $D = 0.10$)

Fig. 3 Resulted spectrogram for different machining setups

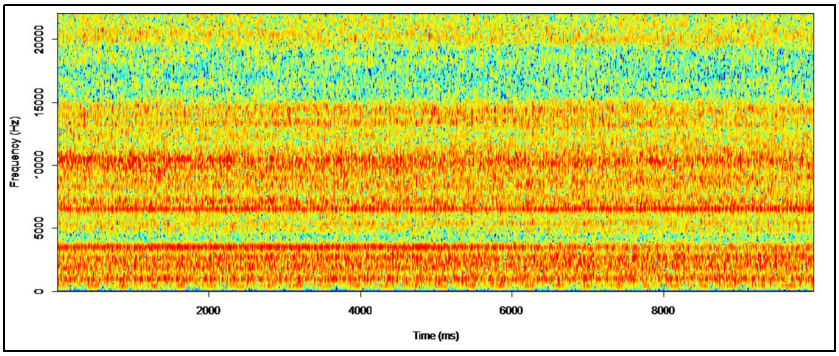

(a) Machining Setup 1 (*Ms1*).

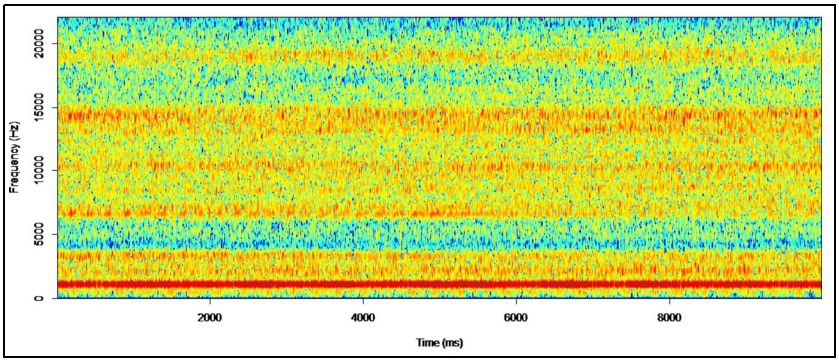

(b) Machining Setup 2 (*Ms2*).

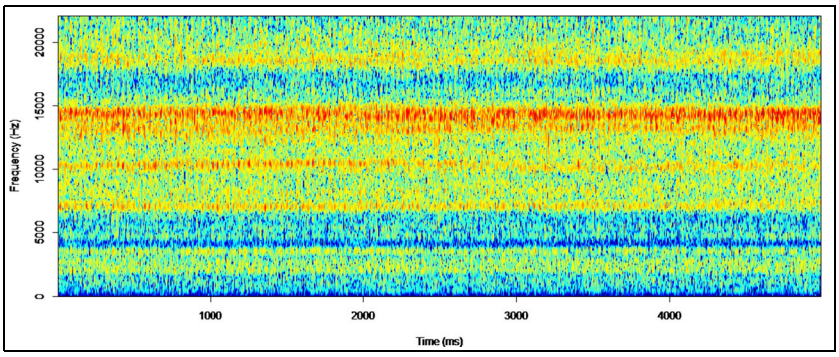

(c) Machining Setup 8 (*Ms8*)

with machining parameters and surface roughness. Table 4 shows that each coefficient presents higher Pearson[1] correlation with different machining parameter, for example, c_1 and c_2 coefficient correlates with material remove rate (*MRR*), and also with all finishing surface roughness parameter (*Ra*, *Ry*, *Rz*, *Rq*, *Rt*, and *Rsm*) presenting higher correlation with maximum peak to valley surface roughness (*Rt*). Already c_5 coefficient, stronger correlation occurs with cutting speed (*CS*) machining parameter. Each coefficient c_m presented in Table 4 is represented by its mean μ_m since standard deviation σ_m presented no strong correlation with any machining parameter or surface roughness, and hence it was omitted.

This correlation presents that the cutting specific energy (related to the MRR) applied to the system is probably transformed in other types of energy like heat (tool edge, work-piece, chip, and air), sound, vibration, and others. In

[1]The Pearson product-moment correlation is used to assess the strength and direction of association between two continuous variables that are linearly related. Its coefficient, r, indicates the strength and direction of this relationship and can range from -1 for a perfect negative linear relationship to +1 for a perfect positive linear relationship. A value of 0 (zero) indicates that there is no relationship between the two variables.

Table 4 Correlation analysis between scores, machining setup parameter and surface roughness

MFCC	CS	F	D	MRR	Ra	Ry	Rz	Rq	Rt	Rsm
c_1	0.061[b]	*0.594*[a]	*0.563*	*0.781*	*0.595*	*0.665*	*0.629*	*0.607*	*0.685*	*0.419*
	0.457[c]	0.000	0.000	0.000	0.000	0.000	0.000	0.000	0.000	0.000
c_2	-0.069	*-0.703*	*-0.506*	*-0.802*	*-0.649*	*-0.722*	*-0.671*	*-0.662*	*-0.752*	*-0.507*
	0.403	0.000	0.000	0.000	0.000	0.000	0.000	0.000	0.000	0.000
c_3	0.123	*0.430*	0.210	*0.414*	0.228	0.265	0.220	0.235	0.318	0.285
	0.135	0.000	0.010	0.000	0.005	0.001	0.007	0.004	0.000	0.000
c_4	0.440	-0.240	0.334	0.204	-0.040	-0.053	-0.003	-0.048	-0.158	-0.097
	0.000	0.003	0.000	0.012	0.629	0.523	0.974	0.558	0.054	0.238
c_5	*0.673*	0.029	0.437	0.432	0.003	0.037	0.037	0.006	0.018	0.021
	0.000	0.722	0.000	0.000	0.974	0.657	0.656	0.938	0.831	0.803
c_6	*0.566*	0.001	-0.098	0.058	-0.052	-0.126	-0.066	-0.063	-0.216	0.093
	0.000	0.995	0.233	0.483	0.528	0.125	0.422	0.445	0.008	0.260
c_7	-0.069	0.029	0.077	0.106	-0.081	-0.058	-0.039	-0.072	-0.037	-0.135
	0.403	0.720	0.349	0.196	0.327	0.477	0.637	0.378	0.650	0.099
c_8	*-0.607*	0.207	-0.228	-0.173	0.063	0.076	0.051	0.068	0.165	-0.031
	0.000	0.011	0.005	0.034	0.447	0.358	0.534	0.411	0.043	0.707
c_9	*-0.562*	-0.021	-0.361	-0.296	-0.032	-0.066	-0.069	-0.036	-0.043	0.010
	0.000	0.799	0.000	0.000	0.694	0.424	0.403	0.666	0.602	0.900
c_{10}	0.013	0.239	-0.032	0.110	0.291	0.237	0.237	0.280	0.206	0.346
	0.874	0.003	0.696	0.179	0.000	0.003	0.004	0.001	0.011	0.000
c_{11}	*0.616*	-0.037	0.271	0.324	0.062	0.062	0.065	0.059	0.014	0.159
	0.000	0.653	0.001	0.000	0.453	0.448	0.433	0.472	0.867	0.052
c_{12}	*0.614*	0.052	0.334	0.363	-0.020	0.025	0.012	-0.013	0.024	0.006
	0.000	0.529	0.000	0.000	0.808	0.758	0.880	0.872	0.772	0.946

[a]Italic values represent higher Pearson correlations that are statistically significant (P-value $< 5\ \%$)

[b]Pearson correlation

[c]P-value

this case, the part of the energy transferred to the acoustic signal can be identified by MFCC, what makes this feature a good component for applying in monitoring methods.

Figure 4 illustrates the experimental results for 15 replicas as well as determines how strongly negative were the correlations between second MFCC (c_2) and surface

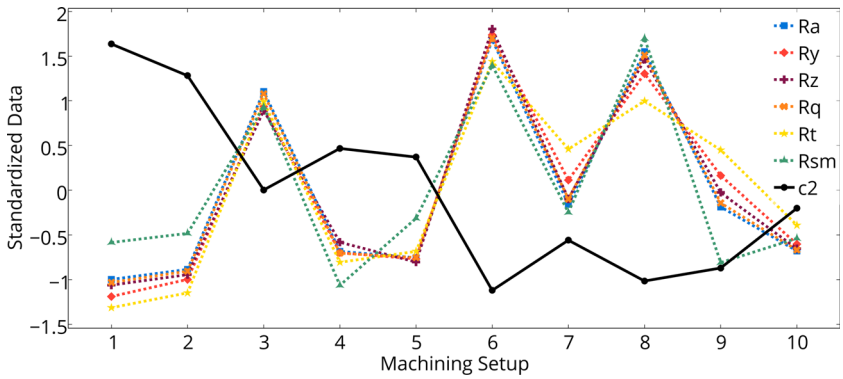

Fig. 4 Line plots for standardized surface roughness parameters and Mel-frequency cepstral coefficient (c_2)

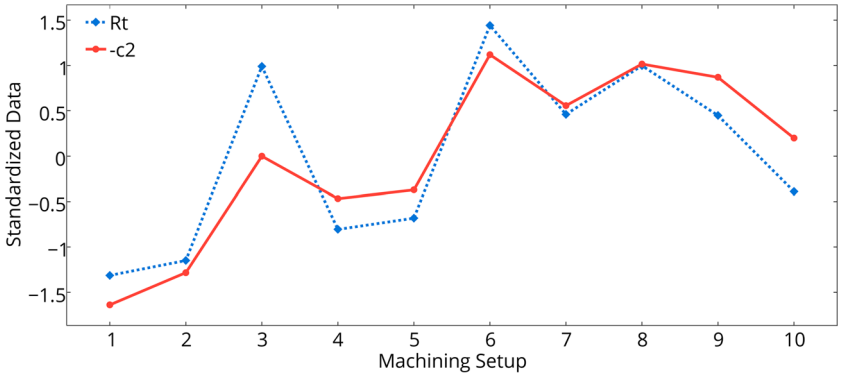

Fig. 5 Line plots for standardized surface roughness (*Rt*) and Mel-frequency cepstral coefficient ($-c_2$)

roughness parameters. It highlights this correlation showing that for all machining setups, when the surface roughness increases, the MFCC has the same behavior but in the opposite way, presenting a negative correlation. Also, Fig. 5 highlights that c_2 level follows surface roughness *Rt* with a higher correlation, as presented before on Table 4.

Two replicates were randomly selected for applying the response surface analysis in the surface roughness parameters *Ra*, *Ry*, *Rz*, *Rq*, *Rt*, and the Mel-frequency cepstral coefficient c_2. Table 5 shows regression coefficients, R-Sq (adj.) and Anderson-Darling normality test for residuals of each response. The results have presented not only adequate coefficients of determination (above 95 %, exception for $R_t = 86.13$ %), but also enough evidence to affirm that residuals are following normal distributions. As can be observed in Table 5, feed rate F was the most important factor explaining the average behavior of surface roughness parameters and was also one of the most import factors explaining the second MFCC. Reference [33] showed that the surface roughness is strongly correlated to feed rate (F) so this similarity might be one of the reasons why strong correlations between surface roughness parameters and MFCC were observed. On the other hand, the depth of cut D had higher impact on MFCC coefficient than on mechanical properties. Hence, practitioners must dedicate close attention to this control variable in order to guarantee the reliability of decision-makings for process monitoring. Probably, this is the main reason why the correlation structure was not even stronger.

Finally, Fig. 6 graphically represents the response surface models comparing two surface roughness parameters (*Ry* and *Rt*) to the second Mel-Frequency Cepstral Coefficient c_2 and their negative relationship are clearly visualized, mainly due to the contour plots for $F \times CS$ and $D \times F$.

Table 5 Regression coefficients and coefficients of determination

	Ra	*Ry*	*Rz*	*Rq*	*Rt*	c_2
Constant	*0.185*[a]	*1.387*	*0.958*	*0.236*	2.133	*-32.234*
CS	*0.074*	*0.202*	*0.24*	*0.079*	0.074	*2.765*
F	*0.169*	*0.746*	*0.616*	*0.194*	*0.773*	*-9.278*
D	*-0.053*	-0.035	*-0.111*	*-0.051*	0.075	*-10.073*
CS^2	*0.075*	*0.33*	*0.267*	*0.084*	0.201	0.091
F^2	*0.014*	0.002	0.044	0.015	-0.123	0.78
D^2	*0.057*	*0.198*	*0.172*	*0.062*	0.162	*3.079*
$CS \times F$	*0.077*	*0.197*	*0.266*	*0.081*	0.043	*5.743*
$CS \times D$	-0.01	-0.051	-0.052	-0.011	-0.009	0.743
$F \times D$	*-0.063*	-0.081	*-0.159*	*-0.063*	0.046	*-5.759*
S	0.013	0.135	0.085	0.018	0.262	1.283
R-Sq(adj)	99.27 %	95.79 %	97.62 %	98.80 %	86.13 %	98.70 %
Normality test	0.433[b]	0.268	0.117	0.118	0.328	0.382
for residuals	0.273[c]	0.646	0.988	0.988	0.492	0.365

[1] Italic values represent the significant terms in the models (P-value < 5 %)

[a] Anderson-Darling test statistic

[b] P-value

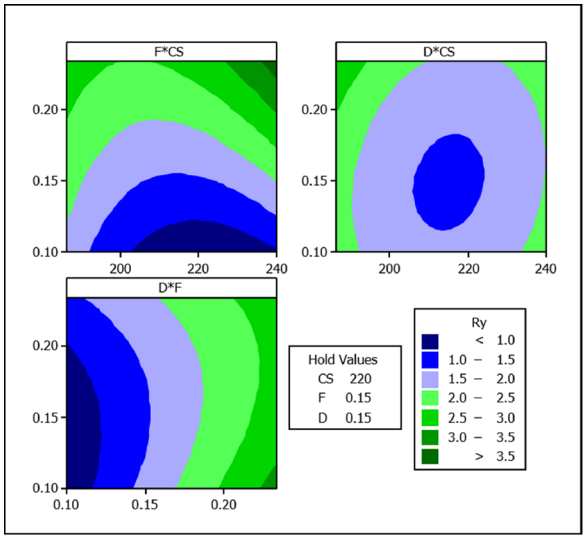

(a) Ry

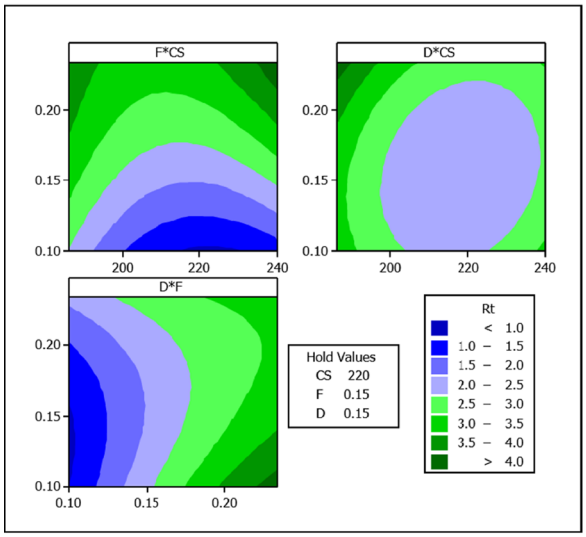

(b) Rt

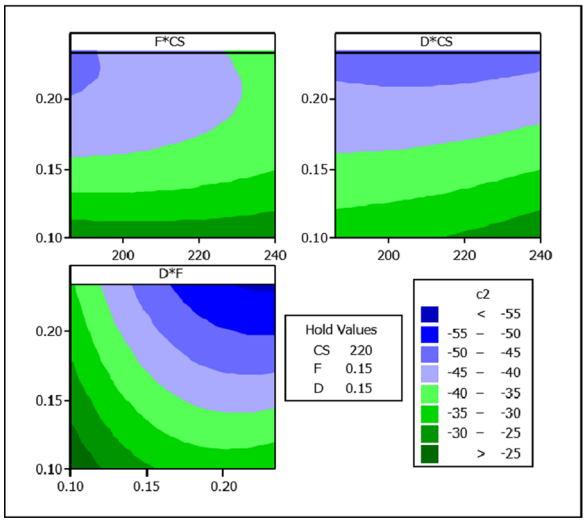

(c) MFCC c_2

Fig. 6 Contour plots for for surface roughness and *Mel* coefficient

6 Conclusions

During the last years, notable efforts have been made to develop reliable and industrially applicable machining monitoring systems based on different types of sensors, especially indirect methods that does not required to interrupt the machining process. The main focus of this work is the establishment of correlation between audible sound energy and surface roughness in order to allow the effective use of such feature in quality monitoring methods.

In order to characterize the audible sound energy signals emitted by different cutting conditions during turning of AISI-5210 hardened steel, machining parameters were varied based on a CCD and the corresponding acoustic signals were detected and processed in the frequency domain by calculating the Mel-Frequency Cespstral Coefficients.

Pearson correlation analysis was performed to evaluate the linear relationship between MFCC levels and machining parameters where it was possible to detect strong correlations such as c_1 and c_2 with material removal rate (*MRR*) and all surface roughness, and also c_5 with cutting speed (*CS*). To better understand such relationship, graphical analysis was used where the linear relationship was highlighted since machining parameters change resulted proportional changes in the MFCC levels.

Also, a response surface analysis was applied in the surface roughness parameters *Ra*, *Ry*, *Rz*, *Rq*, *Rt* and the Mel-frequency cepstral coefficient c_2 and showed that feed rate *F* was the most important factor explaining the average behavior of surface roughness parameters and was also one of the most import factors explaining the second *Mel* coefficient, which explains the strong correlations between surface roughness parameters and MFCC. Those observations lead us to conclude that features obtained from sound energy can be applied in quality monitoring process methods.

Further works can be performed in order to test this approach for different machining process, such as milling and drilling. Classification methods based on ANN and also Gaussian Mixture Models (GMM) can be tested in order to propose monitoring methods using MFCC extracted from sound energy.

Acknowledgments This research was supported by CAPES under process number BEX 3203/15-8. Thanks also to the Brazilian governmental agencies of CNPq and FAPEMIG.

References

1. Özel T, Karpat Y (2005) Predictive modeling of surface roughness and tool wear in hard turning using regression and neural networks. Int J Mach Tools Manuf 45(4–5):467–479, 4. doi:10.1016/j.ijmachtools.2004.09.007

2. Teti R, Jemielniak K, ODonnell G, Dornfeld D (2010) Advanced monitoring of machining operations. CIRP Ann Manuf Technol 59(2):717–739, 1. doi:10.1016/j.cirp.2010.05.010
3. Bernhard S (2002) On-line and indirect tool wear monitoring in turning with artificial neural networks: a review of more than a decade of research. Mech Syst Signal Process 16(4):487–546, 7. doi:10.1006/mssp.2001.1460
4. Dimla DE Sr., Lister PM (2000) On-line metal cutting tool condition monitoring. i : force and vibration analyses. Int J Mach Tools Manuf 40:739–768
5. Xiqing Mu, Chuangwen Xu (2009) Tool wear monitoring of acoustic emission signals from milling processes. In: 2009 First international workshop on education technology and computer science, pp 431–435. IEEE. doi:10.1109/ETCS.2009.105
6. Kasban H, Zahran O, Arafa H, El-Kordy M, Elaraby SMS, Abd El-Samie FE (2011) Welding defect detection from radiography images with a cepstral approach. NDT & E International 44(2):226–231, 3. doi:10.1016/j.ndteint.2010.10.005
7. Chen B, Chen X, Li B, He Z, Cao H, Cai G (2011) Reliability estimation for cutting tools based on logistic regression model using vibration signals. Mech Syst Signal Process 25(7):2526–2537, 10. doi:10.1016/j.ymssp.2011.03.001
8. Rubio EM, Teti R (2010) Process monitoring systems for machining using audible sound energy sensors. In: Aized T (ed) Future Manufacturing Systems, pp 217–235. Sciyo. doi:10.5772/55601, (to appear in print)
9. Mannan MA, Kassim AA, Ma J (2000) Application of image and sound analysis techniques to monitor the condition of cutting tools. Pattern Recogn Lett 21(11):969–979, 10. doi:10.1016/S0167-8655(00)00050-7
10. Ai CS, Sun YJ, He GW, Ze XB, Li W, Mao K (2011) The milling tool wear monitoring using the acoustic spectrum. Int J Adv Manuf Technol 61(5–8):457–463, 11. doi:10.1007/s00170-011-3738-z
11. Emerson Raja J, Lim WS, Venkataseshaiah C (2012) Emitted sound analysis for tool flank wear monitoring using hilbert huang transform. International Journal of Computer and Electrical Engineering 4(2). doi:10.7763/IJCEE.2012.V4.460
12. Boutros T, Liang M (2011) Detection and diagnosis of bearing and cutting tool faults using hidden markov models. Mech Syst Signal Process 25(6):2102–2124, 8. doi:10.1016/j.ymssp.2011.01.013
13. Robben L, Rahman S, Buhl JC, Denkena B, Konopatzki B (2010) Airborne sound emission as a process monitoring tool in the cut-off grinding of concrete. Appl Acoust 71(1):52–60. doi:10.1016/j.apacoust.2009.07.004
14. Salgado DR, Alonso FJ (2007) An approach based on current and sound signals for in-process tool wear monitoring. Int J Mach Tools Manuf 47(14):2140–2152. doi:10.1016/j.ijmachtools.2007.04.013
15. Lu M-C, Wan B-S (2012) Study of high-frequency sound signals for tool wear monitoring in micromilling. Int J Adv Manuf Technol:1785–1792, 8. doi:10.1007/s00170-012-4458-8
16. Downey J, OLeary P, Raghavendra R (2014) Comparison and analysis of audible sound energy emissions during single point machining of hsts with pvd ticn cutter insert across full tool life. Wear 313(1–2):53–62, 5. doi:10.1016/j.wear.2014.02.004
17. Lee SS, Chen JC (2003) On-line surface roughness recognition system using artificial neural networks system in turning operations. Int J Adv Manuf Technol 22(7–8):498–509, 11. doi:10.1007/s00170-002-1511-z
18. Khorasani AM, Yazdi MRS (2015) Development of a dynamic surface roughness monitoring system based on artificial neural networks (ann) in milling operation. Int J Adv Manuf Technol:10. doi:10.1007/s00170-015-7922-4
19. Koolagudi SG, Rastogi D, Sreenivasa Rao K (2012) Identification of language using mel-frequency cepstral coefficients (mfcc). Procedia Engineering 38:3391–3398, 1. doi:10.1016/j.proeng.2012.06.392
20. Junqin W, Junjun Y (2011) An improved arithmetic of mfcc in speech recognition system. In: 2011 International conference on electronics communications and control ICECC, pp 719–722. IEEE, DOI doi:10.1109/ICECC.2011.6066676, (to appear in print)
21. Jardine AKS, Lin D, Banjevic D (2006) A review on machinery diagnostics and prognostics implementing condition-based maintenance. Mech Syst Signal Process 20(7):1483–1510, 10. doi:10.1016/j.ymssp.2005.09.012
22. Wang C-C, Kang Y (2012) Feature extraction techniques of non-stationary signals for fault diagnosis in machinery systems. Journal of Signal and Information Processing 03(01):16–25. doi:10.4236/jsip.2012.31002
23. Cohen L (1994) Time Frequency Analysis: Theory and Applications, 1st edn. Prentice Hall
24. Marinescu I, Axinte D (2009) A time-frequency acoustic emission-based monitoring technique to identify workpiece surface malfunctions in milling with multiple teeth cutting simultaneously. Int J Mach Tools Manuf 49(1):53–65. doi:10.1016/j.ijmachtools.2008.08.002
25. Picone JW (1993) Signal modeling techniques in speech recognition. Proc IEEE 81(9):1215–1247. doi:10.1109/5.237532
26. Davis S, Mermelstein P (1980) Comparison of parametric representations for monosyllabic word recognition in continuously spoken sentences
27. Shantha Selva Kumari R, Selva Nidhyananthan S, Anand G (2012) Fused mel feature sets based text-independent speaker identification using gaussian mixture model. Procedia Engineering 30:319–326, 1. doi:10.1016/j.proeng.2012.01.867
28. Dhanalakshmi P, Palanivel S, Ramalingam V (2011) Classification of audio signals using aann and gmm. Appl Soft Comput 11(1):716–723, 1. doi:10.1016/j.asoc.2009.12.033
29. Fahmy MMM (2010) Palmprint recognition based on mel frequency cepstral coefficients feature extraction. Ain Shams Engineering Journal 1(1):39–47, 9. doi:10.1016/j.asej.2010.09.005
30. Dannenberg R (2013) Audacity. http://audacity.sourceforge.net/
31. Paiva AP, Campos PH, Ferreira JR, Lopes LGD, Paiva EJ, Balestrassi PP (2012) A multivariate robust parameter design approach for optimization of aisi 52100 hardened steel turning with wiper mixed ceramic tool. Int J Refract Met Hard Mater 30(1):152–163, 1. doi:10.1016/j.ijrmhm.2011.08.001
32. Montgomery DC (2013) Design and Analysis of Experiments, 8edn. Wiley
33. Tekner Z, Yeşlyurt S (2004) Investigation of the cutting parameters depending on process sound during turning of aisi 304 austenitic stainless steel. Mater Des 25(6):507–513, 9. doi:10.1016/j.matdes.2003.12.011. http://linkinghub.elsevier.com/retrieve/pii/S0261306903002632